

Monitoring the Film Coating Unit Operation and Predicting Drug Dissolution Using Terahertz Pulsed Imaging

LOUISE HO,^{1,2,3} RONNY MÜLLER,⁴ KEITH C. GORDON,⁵ PETER KLEINEBUDDE,⁴ MICHAEL PEPPER,^{2,3} THOMAS RADES,¹ YAOCHUN SHEN,⁶ PHILIP F. TADAY,³ J. AXEL ZEITLER⁷

¹School of Pharmacy, University of Otago, P.O. Box 56, Dunedin, New Zealand

²Cavendish Laboratory, University of Cambridge, Cambridge CB3 0HE, UK

³TeraView Ltd, St. John's Innovation Park, Cambridge CB4 0WS, UK

⁴Institute of Pharmaceutics and Biopharmaceutics, Heinrich-Heine-University, Universitätsstr.1, Düsseldorf D-40225, Germany

⁵Department of Chemistry, MacDiarmid Institute for Advanced Materials and Nanotechnology, University of Otago, P.O. Box 56, Dunedin, New Zealand

⁶Department of Electrical Engineering and Electronics, University of Liverpool, Brownlow Hill, Liverpool L69 3GJ, UK

⁷Department of Chemical Engineering and Biotechnology, University of Cambridge, New Museums Site, Pembroke Street, Cambridge CB2 3RA, UK

Received 12 November 2008; revised 9 February 2009; accepted 17 February 2009

Published online 14 April 2009 in Wiley InterScience (www.interscience.wiley.com). DOI 10.1002/jps.21766

ABSTRACT: Understanding the coating unit operation is imperative to improve product quality and reduce output risks for coated solid dosage forms. Three batches of sustained-release tablets coated with the same process parameters (pan speed, spray rate, etc.) were subjected to terahertz pulsed imaging (TPI) analysis followed by dissolution testing. Mean dissolution times (MDT) from conventional dissolution testing were correlated with terahertz waveforms, which yielded a multivariate, partial least squares regression (PLS) model with an R^2 of 0.92 for the calibration set and 0.91 for the validation set. This two-component, PLS model was built from batch I that was coated in the same environmental conditions (air temperature, humidity, etc.) to that of batch II but at different environmental conditions from batch III. The MDTs of batch II was predicted in a nondestructive manner with the developed PLS model and the accuracy of the predicted values were subsequently validated with conventional dissolution testing and found to be in good agreement. The terahertz PLS model was also shown to be sensitive to changes in the coating conditions, successfully identifying the larger coating variability in batch III. In this study, we demonstrated that TPI in conjunction with PLS analysis could be employed to assist with film coating process understanding and provide predictions on drug dissolution. © 2009 Wiley-Liss, Inc. and the American Pharmacists Association *J Pharm Sci* 98:4866–4876, 2009

Keywords: terahertz pulsed imaging (TPI); coating; controlled release; image analysis; dissolution; unit operations; sustained-release; coating curing

INTRODUCTION

Film coating is generally carried out as the penultimate step to packaging, in the manufacturing processes for tablets.¹ Therefore, it is axiomatic that the quality of the film coating is

Correspondence to: Louise Ho (Telephone: 64-3-479-7275; Fax: 64-3-479-7034; E-mail: louise.ho@otago.ac.nz)

Journal of Pharmaceutical Sciences, Vol. 98, 4866–4876 (2009)
© 2009 Wiley-Liss, Inc. and the American Pharmacists Association

pertinent to the aesthetic and performance properties of the final product.^{1,2} Fast and easy measurements like tablet film coating weight-gain and determination of the amount of coating polymer applied are process signatures most commonly monitored to control the progress of the film coating unit operation and the film coating quality of the batch. However, neither tablet film coating weight-gain, nor the amount of coating polymer applied could afford information on the film coating uniformity, thickness and density; thus they are often inadequate to accurately reflect the progress of the film coating process and predict the *in vitro* dissolution performance of the final product.³⁻⁶

The film coating unit operation has been closely examined using spectroscopic techniques like near-infrared (NIR), X-ray photoelectron (XPS) and Raman spectroscopy to gain a better understanding of the processes in order to achieve a built-in product quality or to improve the product design space.^{7,8} Coupled with multivariate analyses, both Raman and NIR spectroscopy demonstrated their capabilities in investigating the film coating unit operation in a qualitative and quantitative manner.^{3,8-13} Moreover, NIR in particular has been applied to predict drug dissolution. NIR spectra of uncoated carbamazepine tablets were used to predict the dissolution rate using principle component regression (PCR).¹⁴ Similarly a series of statistical models were built, including using partial least squares (PLS) analysis to investigate correlation of the dissolution profiles at five time points (15, 30, 60, 90 and 120 min) with the NIR spectra of uncoated theophylline tablets compressed at different forces.¹⁵ PLS models were also developed from NIR spectra to predict dissolution of uncoated clonazepam tablets at seven time points in three different media.¹⁶ Furthermore, both transmittance and diffused reflectance NIR spectra of uncoated indomethacin tablets were used to construct PCR models to study the effect of varying compression forces on dissolution, in particular correlations to the time required at 75% dissolution and mean dissolution time (MDT).¹⁷ A PCR model was also built using NIR spectra of uncoated theophylline tablets and tablets coated with 2% and 3% ethylcellulose to predict the dissolution time at 50% drug release.¹⁸ Recently, Felton and coworkers¹⁹ in a study using XPS in concert with PCA have demonstrated that images of the film-tablet interface may be obtained to study the relationship between

atomisation air pressure and the thickness of the film-tablet interface. By changing the atomisation air pressure during the coating process, Felton and coworkers¹⁹ were able to establish that higher atomisation air pressure resulted in thinner film-tablet interface, thus highlighting the role of coating process parameters in the physical changes in the tablet-film interface.

Imaging of pharmaceutical solid dosage forms with terahertz radiation ($2-120\text{ cm}^{-1}$) has evolved from a single point (single pixel) measurement capability to fully automated imaging, covering the entire area or selected regions of the sample surface (thousands of pixels depending on the size of the sample).^{20,21} Whilst the fast single point measurement (50 ms) is geared towards on-line applications, the off-line whole surface scan (45 min on a biconvex tablet with an 8 mm diameter and 3 mm height, at a step-size of $200\text{ }\mu\text{m}$) has played an important role in gaining an insight into the coating processes. This can be attributed to the penetration depth of terahertz radiation of up to 5 mm into the sample, which renders non-destructive construction of virtual cross-sections and three-dimensional modelling of the sample structure possible. These are important tools in defect diagnostics (even when the defects are buried below the surface of the coating) and resolving multiple layers of a complex film coating.^{22,23}

Details of the technical set-up and the imaging process have been reported previously.^{24,25} In short, photoconductive semiconductor antennas are used to generate and receive terahertz radiation (which resides in the far-infrared region of the electromagnetic spectrum). The current set-up is time-gated by the arrival of the femtosecond laser beams, where the pump beam excites the emitter to generate pulses of terahertz radiation and the probe beam illuminates the receiver. Most pharmaceutical excipients are either transparent or semitransparent in the far-infrared region. Thus pulses of terahertz radiation can penetrate most coating structures and internal physico-chemical changes are generally visible as echoes in the time domain waveform. This time domain waveform can then be exploited to generate information on film coating thickness, surface roughness and variations in film coating density.⁵ Terahertz pulsed imaging (TPI) has been employed to investigate the film coating quality of commercial products;²¹ analysing batch variability in film coating thickness and detecting coating defects,²² exploring the reason behind a film coating scale-up failure⁴ and assessing the

film coating unit operation upon process scale-up.⁵ In this study we demonstrate how terahertz waveforms can be employed together with multivariate analysis (PLS) to gain a better understanding of the progress of a film coating process and how the information derived can be used to predict drug dissolution of two other batches of sustained-release tablets coated with the same process parameters.

MATERIALS AND METHODS

Coating of Sustained-Release Tablets

Three lab-scale batches were coated using the same process parameters previously described.⁴ Each batch contains 4 kg of tablet cores. These were biconvex tablets, which were 8 mm in diameter and 3 mm in height and weighed around 252 mg. Each tablet core contained 10% (w/w) diprophyllin (API), 0.5% (w/w) magnesium stearate, 5% (w/w) vinylpyrrolidone–vinyl acetate copolymer (Kollidon[®] VA 64) and 84.5% (w/w) lactose monohydrate (Flowlac[®]). The lab-scale batches were coated using a Bohle Film Coater (model BFC5, L.B Bohle, Ennigerloh, Germany) with a 316 mm diameter and 356 mm length-coating pan. A single two-way spray nozzle (type 970/7-1 S75, Düsen-Schlick GmbH, Untersiemau, Germany) was used to spray coating solution. The coating formulation applied was as follows: 50% (w/w) polyvinyl acetate (Kollicoat[®] SR 30 D), 6% (w/w) polyvinyl alcohol–polyethyleneglycol graft copolymer (Kollicoat[®] IR), 0.075% (w/w) polyoxyethylene (20) sorbitan monooleate (Polysorbat 80), 0.3% (w/w) glycerolmonostearate, 0.75% (w/w) triethylcitrate (5.0% (w/w) based on amount of the dry Kollicoat SR) and 42.87% (w/w) deionised water. Ten samples were randomly selected during the coating process of batch I, at 10% increments of the amount of sustained-release polymer applied (1.7, 3.7, 5.2, 7.0, 8.7, 10.5, 12.2, 14.0, 15.7 and 17.5 mg/cm²) and from the finished product coated at the final coating level of 17.5 mg/cm² and cured for 48 h at 60°C. Ten more samples were randomly collected from the finished product (after curing) of batch I for further validating the PLS model. In addition, 10 tablets were also randomly sampled from the finished product of batches II and III for prediction of dissolution.

Terahertz Pulsed Imaging

All tablets were imaged with the TPI Imaga 2000 (TeraView, Cambridge, UK) prior to dissolution

testing. The tablet imaging process has been previously described in detail.²² Briefly, a 670 nm laser was used to build the topological model of the tablet. Once the sample had been scanned in front of the 670 nm laser gauge, the robotic arm presented the sample to the terahertz gauge for terahertz mapping. The tablet central band was mapped out in point-to-point mode with 200 µm steps. The tablet central band was chosen as it has previously been shown to be the weakest area of the film coat and is dissolution rate determining.^{3,26} For this study, an average terahertz time domain waveform (corresponding to an optical delay length of –1 to 1 mm) over 1,200 pixels around the central band was extracted from each tablet for PLS analysis. The entire terahertz waveform (from –1 to 1 mm) was employed in the analysis. The optical delay in the time-domain was converted from seconds into millimetres to allow for quick coating thickness interpretations.

Dissolution Studies

Dissolution analysis was performed conforming to the USP guidelines for sustained-release dosage forms. A paddle dissolution apparatus (AT 7smart On-line, Sotax, Allschwil, Switzerland) was used with a paddle rotational speed of 100 rpm. The dissolution medium was 900 mL of water in each beaker and the temperature was kept constant at 37°C. A UV spectrometer (Lambda 2 UV/Vis, Perkin-Elmer GmbH, Düsseldorf, Germany) was employed to determine the drug concentration in-line. Automatic sampling at 1 min intervals was carried out through the entire dissolution process (25 h). The UV detection wavelength was set at 272 nm—the maximum absorption of diprophyllin in an aqueous solution. The MDT was derived from the dissolution profiles as the model independent dissolution parameter and included in the PLS analysis. Differing from other model independent dissolution parameters like $t_{20\%}$, $t_{50\%}$ and $t_{80\%}$, MDT takes the shape of the dissolution curve into account and therefore is more robust in reflecting the true dissolution performance of sustained-release tablets.²⁷ The MDT was calculated from the following equation.²⁸

$$\text{MDT} = \frac{\int_0^{\infty} t W_d(t) dt}{\int_0^{\infty} W_d(t) dt}$$

where, $W_d(t)$ is the cumulative amount of drug dissolved and t the time interval.

PLS Analysis of Terahertz Waveforms

Terahertz waveforms contain film coating quality information including film coating thickness, variations in film coating density, surface roughness and film coating uniformity at the film/core interface. Traditionally (Fig. 1) this information is extracted from parts of the terahertz waveform; by determining the distance between the surface reflection and interface reflection for coating thickness and other terahertz parameters like terahertz electric field peak strength (TEFPS) and terahertz interface index (TII) to investigate surface roughness and variations in coating density.^{4,26} We have demonstrated the importance of these terahertz parameters to MDT through univariate analysis.^{4,5} Here, for the first time, we explore multivariate analysis by employing PLS regression, where the entire waveform was taken into account and the regression algorithm cross-correlates the \mathbf{X} matrix (terahertz waveforms) and the y -variable (MDT).²⁹ This cross-correlation between the \mathbf{X} matrix and the y -variable ensures any variances from the terahertz waveforms (\mathbf{X} matrix) described in the PLS model are related to the changes in the MDT.³⁰

PLS regression analysis (The Unscrambler v 9.8, Camo, Oslo, Norway) was performed where the terahertz waveforms (\mathbf{X} matrix) of all tablets imaged were correlated to the MDT obtained from

subsequent dissolution testing on the same tablets (this was possible as TPI is a nondestructive technique). PLS algorithm directly uses the y -variable to decompose the \mathbf{X} matrix, deducing the loading-weights matrix \mathbf{W} . This \mathbf{W} matrix is then used as inputs for calculating the \mathbf{X} space, \mathbf{T} scores matrix.³⁰ Thus the PLS regression model achieves \mathbf{X} matrix and y -variable interdependently by maximising the (\mathbf{t}, \mathbf{y}) covariance to reach the optimum number of PLS components (PCs) that describe terahertz waveforms in relation to the respective MDT (and *vice versa*) adequately. Further details of the mathematical algorithms are available in the literature.²⁹⁻³¹

Model Development

From batch I, a minimum of five tablets from each sampling interval (at 1.7, 3.7, 5.2, 7.0, 8.7, 10.5, 12.2, 14.0, 15.7, 17.5 mg/cm² amounts of polymer applied) and from the final cured tablets (finished product) were included in the \mathbf{X} matrix. This PLS model was then implemented to predict the MDTs of the finished product from other lab-scale coated batches.

In this study, the terahertz waveform from the sample depicts meaningful information on film coating surface roughness and variations in coating density.^{4,22} All terahertz waveforms were preprocessed with signal deconvolution. This signal deconvolution deals with the baseline shifts and any instrumental dependency so that any nonspecific noise is removed. A flow diagram of the deconvolution process is presented in Figure 2. Further to this, a variety of other preprocessing methods were examined, including the scaling methods: mean centring (MC) and unit variance in conjunction with MC scaling (UV). Preprocessing subsequent to the signal deconvolution described above was kept to a minimum. Initial trials with more sophisticated methods such as standard normal variate transformation (SNV) were investigated. These did not appear to improve our modelling quality.

Full cross-validation was carried out on the calibration set. The quality of the model was assessed with the following parameters: R_{cal}^2 (correlation of determination on the calibration set), R_{val}^2 (correlation of determination on the validation set), root mean square error of calibration (RMSEC) and root mean square error of cross validation (RMSECV). R_{cal}^2 shows how well the terahertz waveforms and MDT are correlated in

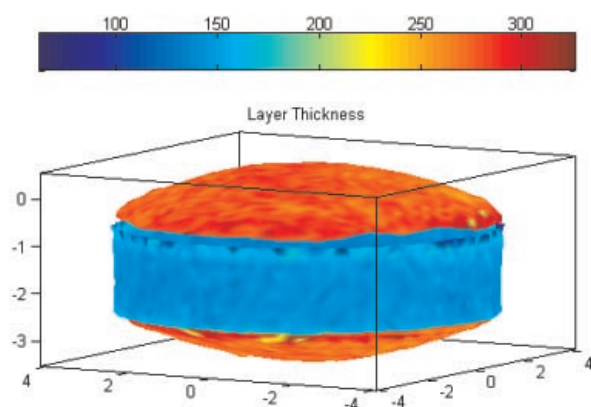


Figure 1. A 3D terahertz tablet scan of a round, biconvex tablet. The scales in the x , y and z directions are in mm. The colour scale bar depicts layer thickness and the unit is in μm .

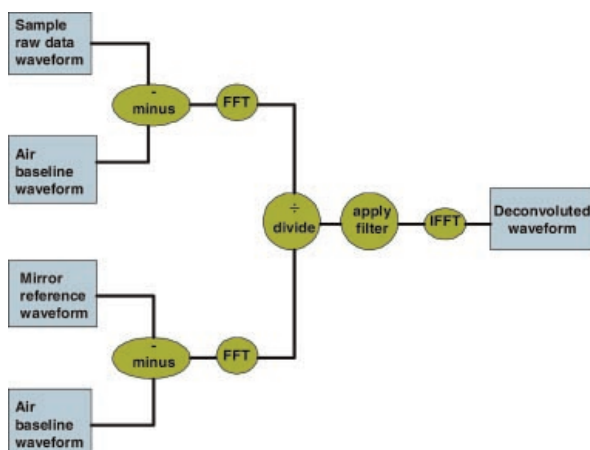


Figure 2. Terahertz time domain signal deconvolution. FFT stands for fast Fourier transformation and IFFT stands for inverse fast Fourier transformation.

the calibration model, while R_{val}^2 indicates the predictive ability of the PLS model.^{29,30} Generally a model is of a high quality and has robust predictive ability when; R_{cal}^2 and R_{val}^2 are high (close to 1), RMSEC and RMSECV are low, the correlation coefficients (R_{cal}^2 and R_{val}^2) are similar to each other and RMSEC is of similar magnitude as that of RMSECV.²⁹

RESULTS AND DISCUSSION

PLS Model—Evaluation of the Scaling

The data for the PLS analyses are presented in Table 1. These data show that scaling the waveform with either UV or MC methods has little effect on the model. UV scaling is generally recognised as the most objective scaling approach to give all variables relatively similar footing in the subsequent multivariate analysis, especially when variables are expressed in different units.^{29,30} UV scaling ensures that each variable

in the \mathbf{X} matrix has equal variance by attaining the standard deviation (S_k) for each column (variable) for the calculation of the scaling weight ($1/S_k$), which is then multiplied with each column of the \mathbf{X} matrix.^{29,30} However this scaling step was not advantageous in this study. All the variables in the terahertz waveforms were of the same unit (in terahertz signal/a.u.) and the column ‘spread’ in each variable of the terahertz waveforms in fact represented the ‘real spread’ of the coating quality within the batch. The deconvoluted terahertz waveforms are extremely sensitive to any physicochemical changes in the film coating.²⁵ Consequently, slight changes encoded in the terahertz waveform usually express coating quality related information.⁴

Additionally, all samples were randomly selected at each sampling interval during the coating process and from the finished cured product. This assured the sample set included tablet coatings with defects that may subsequently result in abnormal dissolution profiles for a fair representation of the quality of the batch. It was thus important to keep the \mathbf{X} -column (variable) ‘spread’ in order to build not only a good quality model but also a working model that was robust enough to predict the subsequent dissolution from products of the same batch and reflect the dissolution behaviour of products from other batches accurately.

Both the unscaled and the MC scaled models expressed a R_{cal}^2 of 0.92 and 0.91 for R_{val}^2 . The calibration error/RMSEC was 0.31 h (MDT range = 3.21–5.61 h) and the prediction error/RMSECV was 0.34 h (Fig. 3). The calibration and validation correlation of determination values were similar, with RMSEC and RMSECV both lying within 10% of each other, indicating the model generated is of good quality. In comparison with a previous NIR dissolution prediction study using PLS models, our PLS models showed much higher similarity between the calibration and validation correlation coefficients. Our best fit values agreed with the optimal values in Freitas et al.,¹⁶ with a much more extensive coverage of

Table 1. Effect of Different Scaling Methods for Terahertz Waveforms on the Quality of the Subsequent PLS Models

Pre-Processing Method	Scaling	PLS Factors	R_{cal}^2	R_{val}^2	RMSEC (h)	RMSEP (h)
Deconvolution	None	2	0.92	0.91	0.31	0.34
	UV	2	0.94	0.92	0.27	0.30
	MC	2	0.92	0.91	0.31	0.34

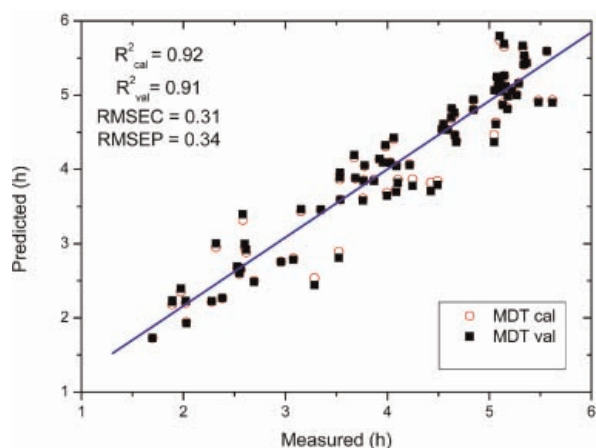


Figure 3. Measured versus predicted MDT from the nonscaled PLS model. Both calibration and validation data points are presented here.

the dissolution profile (using MDT as the y -variable instead of a single time point in the dissolution profile). Since MC scaling added no additional benefit in improving the model quality, the unscaled model was used to further understand the coating process and prediction of the MDT data of two other lab-scale batches.

PLS Assisted Coating Process Understanding

The PLS dissolution prediction model was built with two PCs. Two PCs were chosen so that the model maximised the relationship between terahertz waveforms and MDT values without over fitting.³⁰ The first component (PC1) explained 69% of the information in the terahertz waveforms and 88% of the MDT data. In addition, the second component (PC2) depicted 8% of the terahertz information and 4% the dissolution information. The \mathbf{X} loading weights indicate the regions of the terahertz waveform that have contributed towards each PC.²⁹

PC1 mainly illustrated the changes in the TEFPS as the coating process progressed (Fig. 4). TEFPS is the ratio of the amplitude of the sample surface reflection over the amplitude of the surface reflection from a reference mirror. This was well described by the two positive and one negative peaks in the PC1 loadings, characterising the main changes in the surface reflection of the terahertz waveforms as the coating process

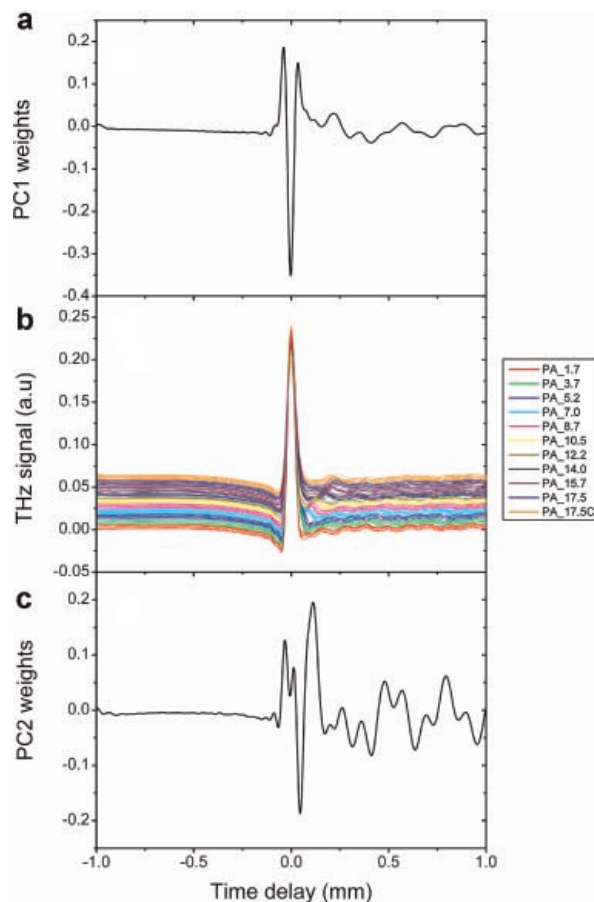


Figure 4. PLS loading-weights for PC1 (a), PC2 (c) and the terahertz waveforms (b) collected at 10% increments of the amount of coating polymer applied. PA is the amount of polymer applied in mg/cm^2 . C stands for cured tablets. The terahertz waveforms are offset for clarity.

progressed. TEFPS describes variations in film coating density and the degree of surface roughness which are both important factors governing the dissolution behaviour.^{4,22} The scores plot showed that PC1 (TEFPS) alone can trace the coating progress reasonably well—spreading from tablets coated at the lowest polymer level ($1.7 \text{ mg}/\text{cm}^2$) from the left moving towards tablets coated with the highest polymer level ($17.5 \text{ mg}/\text{cm}^2$) on the right (Fig. 5). This distribution in general, followed the changes in film coating refractive index as a result of the film formation and effectively trailed the changes in the film coating density during the coating process.⁵ Moreover, the distribution characterised by PC1

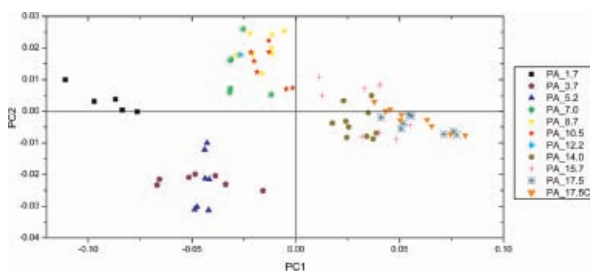


Figure 5. Scores plot of tablets sampled from batch I at 10% increments of the amount of coating polymer applied and from the finished product. PC1 and PC2 together explained 77% of the variation in the terahertz waveforms and 92% of the variation in the MDT data. PC1 traces the coating progress from the lowest polymer level on the left to the highest polymer level on the right; whilst PC2 mainly differentiates the 3.7 and 5.2 mg/cm² cluster from the rest of batch.

in the scores plot did not show a consistent growth pattern, indicating the extensive film coating variability within the batch and the presence of film coating surface roughness.^{5,26}

PC2 primarily differentiated the 3.7 and 5.2 mg/cm² cluster from the rest of the tablets coated at other polymer levels (Fig. 5). As previously illustrated, the time delay position of the interface reflection is important for the calculation of coating thickness.⁵ However, for tablets coated at 1.7, 3.7 and 5.2 mg/cm², the coating/core interface reflection was not clearly resolved as the coating thickness was under 38 μm (the current TPI axial resolution). Instead, exhibiting 'flattening' of the postsurface reflection dip (at 0.04 mm time delay) for tablets coated at 1.7 mg/cm² and the 'emergence' of partially formed interface peaks for tablets coated at 3.7 and 5.2 mg/cm² (Fig. 6a). For clarity, this 'emergence' of the interface reflection peak is also depicted in the schematic diagram in Figure 7. This schematic diagram illustrates the convolution of the surface reflection and the interface reflection at very thin coating thicknesses below the resolution limit of the TPI system. Waveforms for tablets coated at 1.7 and 3.7 mg/cm² correspond to waveforms in Figure 7a and b respectively. Moreover, waveforms for tablets coated at 5.2 mg/cm² share resemblance to waveforms in Figure 7c.

The negative peak at 0.04 mm and the positive peak at 0.11 mm time delay in the PC2 loading-weights plot detected the difference between the partially formed and the complete interface reflection in the waveforms (Fig. 4). Hence PC2

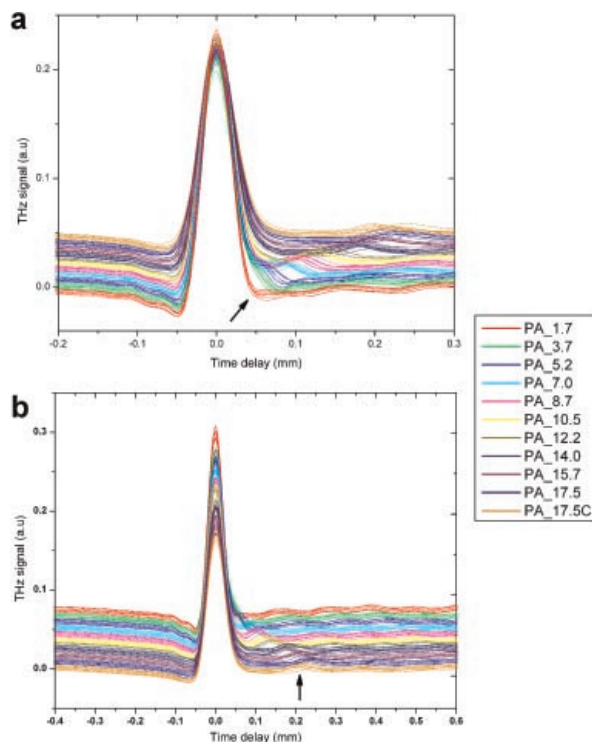


Figure 6. Terahertz waveforms of all samples from batch I. PA is the amount of polymer applied in mg/cm². C stands for cured tablets. The changes in the postsurface reflection dip (at 0.04 mm time delay) are indicated by an arrow in (a). The shift in the interface reflection for tablets after curing is indicated by an arrow in (b). The terahertz waveforms are offset for clarity.

was able to harvest information on the formation of the film coating both below and above the TPI axial resolution and separated out the 3.7 and 5.2 mg/cm² cluster from tablets coated at 7.0 mg/cm² and upwards (the coating thickness was above 38 μm for tablets coated at 7.0 mg/cm²). The fact that PC2 could characterise the formation of film coating below the current axial resolution, extended the breadth of the design space for monitoring the film coating unit operation.⁵ It is important to note nevertheless, that the film coating formation on tablets coated at 1.7 mg/cm² was not characterised by PC2, but PC1 alone. Although PC1 mainly illustrated the changes in the TEFPS, it also partly described the shifts in the time delay position of the interface reflections as the coating process progressed (Fig. 4). Hence PC1 also depicted some information on the growth of coating thickness. Similarly, in addition to representing the coating thickness information on

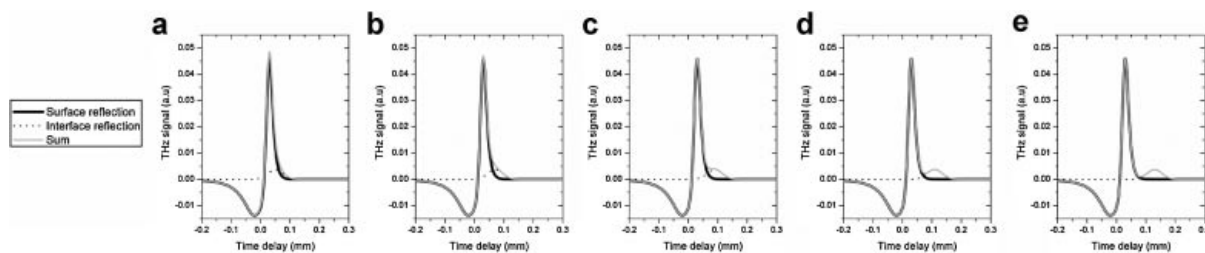


Figure 7. Convolution of the surface and interface reflections at very thin coating levels. The solid black line represents surface reflection whilst the dotted black line represents the interface reflection. The resultant terahertz waveform (solid light grey line) is the sum of the surface and interface reflections.

the lower polymer levels, PC2 also represented some information on TEFPS. As aforementioned, TEFPS is characterised by the surface reflection at 0 mm time delay. At this position, PC2 was above 0 loading weights as shown in Figure 4. Therefore the effect of TEFPS (describes variations in film coating density and surface roughness) and coating thickness in the two PCs are not mutually exclusive and both are related to the changes observed in MDT. This finding with the PLS analysis is consistent with our previous univariate analysis study,⁵ where it was indicated that coating thickness may not have been the sole factor that attributed to the changes in the MDT; thus both terahertz parameters (TEFPS and coating thickness) should be taken into account as important process signatures when considering the design space for analysing sustained-release tablets.

Prediction of MDT

Ten additional samples from the finished product (cured tablets coated at the final polymer level of 17.5 mg/cm²) were selected from batch I to further validate the PLS model. These tablets were subjected to terahertz imaging to obtain the necessary average waveforms from the tablet central bands to implement into the PLS model for the prediction of the subsequent MDT values. To validate the predicted MDT values, conventional dissolution tests were carried out on the same 10 tablets post terahertz imaging. The average dissolution profiles from conventional dissolution testing for batches I, II and III are depicted in Figure 8. The average MDT predicted and the reference results (obtained from dissolution testing) are shown in Table 2, excluding data from one tablet that was lost to a mechanical problem

during dissolution testing. A two-tailed, paired *t*-test was performed and a *p*-value of 0.07 was calculated. The *p*-value was above the null hypothesis $\alpha=0.05$, indicating no statistically significant difference between the predicted and reference means in MDT. Although this demonstrated the desirable capability of predicting the drug dissolution with the terahertz PLS model, it is interesting to note that the average predicted values were, on the whole, lower than that of the reference average MDT values generated from dissolution testing (Tab. 2). This may be due to sample selection and preparation for the PLS model. The PLS model was built largely on uncured tablets from batch I whilst the additional 10 samples selected for validation were cured tablets from the finished product. Furthermore, tablets from batches II and III for dissolution prediction were also cured.

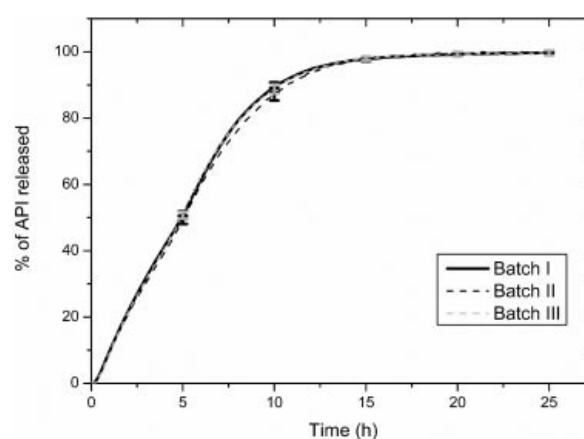


Figure 8. Average dissolution profiles (drug release vs. time) for batches I, II and III. Solid black line—Batch I; dotted black line—Batch II; dotted light grey line—Batch III.

Table 2. Average Predicted and Reference MDT Values. Predicted MDT Values Were Those Derived Using the PLS Model for All Three Batches and Reference Values Were Those Obtained from Conventional Dissolution Testing Subsequent to Terahertz Imaging

	Predicted MDT (h)	Reference MDT (h)
Batch I ($n = 9$)		
Average \pm SD	5.25 ± 0.24	5.43 ± 0.17
t -test p -value = 0.07 ($\alpha = 0.05$)		
Batch II ($n = 10$)		
Average \pm SD	5.35 ± 0.13	5.56 ± 0.19
t -test p -value = 0.07 ($\alpha = 0.05$)		
Batch III ($n = 10$)		
Average \pm SD	5.14 ± 0.22	5.42 ± 0.23
t -test p -value = 0.01 ($\alpha = 0.05$)		

Using samples from batch I as an example, the coating thickness was lower and the coating density was higher for the cured tablets when compared to the uncured tablets coated at the same polymer level (17.5 mg/cm^2). The coating thickness was derived from the distance between the surface reflection and the interface reflection between the film coating and the core.²² It was visible that the interface reflection of the cured tablets shifted to the left of that of the uncured tablets with the same amount of polymer applied (Fig. 6b). Using the following equation $2d_{\text{coat}} = \Delta t c/n$ (Δt is the time delay between the terahertz reflections, c is the speed of light and n is the refractive index of the coating matrix), the coating thickness (d_{coat}) of each waveform was determined for both cured and uncured groups.²² Cured tablets on average were around $7 \text{ }\mu\text{m}$ thinner than that of the uncured tablets. With a similar surface roughness observed around the central band of all tablet examined, a difference of 0.3% in TEFPS (expressed in %) on the cured (16.9%) and uncured (16.6%) tablets was observed. This inferred the film coating density for the cured tablets was higher, which concurred with the lower film coating thickness observed.⁴ Higher film coating density after curing would theoretically lead to slower water permeability into the film and a longer MDT should be expected.^{4,5} The average MDT for the cured tablets (5.33 h) was slightly longer (0.11 h) than the uncured tablets (5.22 h) coated at 17.5 mg/cm^2 . If the PLS model was built solely from cured tablets at each 10% increments of polymer interval, one would expect the predicted MDT to be longer and thus closer to

the reference values derived from the finished product (cured tablets). Further research is currently in progress to investigate the effect of curing on the subsequent dissolution more in-depth.

The same relationship between predicted and reference MDT values was also observed with batches II and III, where the majority of the PLS predicted MDT values were slightly lower than those of the reference values. A two-tailed, paired t -test was also carried out, which yielded a p -value of 0.07 (null hypothesis $\alpha = 0.05$) for batch II. This showed good agreement between the terahertz predicted and reference MDT values, confirming that not only the terahertz PLS model was capable of predicting the MDT values of tablets from the same batch, but also robust enough to predict the MDT values of tablets of other batches coated with the same process parameters and under similar environmental conditions. Batch III was coated with the same process parameters as the other two batches, but at a lower relative humidity (RH). During the film coating process, the RH in the coating drum for batch III was much lower in comparison to the other two batches and it eventually dropped below 20% RH at the end of the coating process. The RH for batches I and II was kept above 25% RH throughout the coating process. The inlet and outlet air temperatures were also monitored during the coating process. Whilst both of these parameters were similar between the three batches, batch III was coated on a hot summer day where the RH in the ambient air was already lower than the other 2 days when batches I and II were coated. The PLS model successfully detected this larger coating variability in batch III, where the t -test p -value was 0.01 (null hypothesis $\alpha = 0.05$). This result demonstrates the sensitivity of the terahertz PLS model to subtle physicochemical changes in the film coating as the consequence not only of changes in the coating process parameters but also the environmental conditions under which the batch was coated.

CONCLUSIONS

Multivariate analysis was employed in this study. By coupling the conventional dissolution parameter (MDT) to terahertz waveforms, the resultant terahertz PLS model provided insight into not only physicochemical changes in the film coating (as a consequence of changes in the

environmental conditions), but also predictions on the corresponding *in vitro* dissolution whilst the tablets were still intact. MDTs obtained from conventional dissolution testing were correlated to terahertz waveforms on tablets sampled from batch I. Using the terahertz PLS model, the MDT values for tablets from batch II was successfully predicted in a nondestructive manner. The PLS model was also sensitive to the increased coating variability in batch III, possibly as a result of environmental changes during the film coating process. The concept presented in this study potentially opens new avenues to achieving a greater understanding and better control of the coating unit operation.

ACKNOWLEDGMENTS

J. Axel Zeitler would like to acknowledge funding from the Research Councils UK Basic Technology Programme.

REFERENCES

- Rantanen J. 2007. Process analytical applications of Raman spectroscopy. *J Pharm Pharmacol* 59:171–177.
- Cole GC. 1995. Introduction and overview of pharmaceutical coating. In: Cole G, Hogan J, Michael A, editors. *Pharmaceutical coating technology*. 1st edition. Philadelphia: Taylor & Francis Ltd. pp. 1–5.
- Perez-Ramos JD, Findlay WP, Peck G, Morris KR. 2005. Quantitative analysis of film coating in a pan coater based on in-line sensor measurements. *AAPS PharmSciTech* 6:E128–E136.
- Ho L, Müller R, Gordon KC, Kleinebudde P, Pepper M, Rades T, Shen Y-C, Taday PF, Zeitler JA. 2008. Applications of terahertz pulsed imaging to sustained-release tablet film coating quality assessment and dissolution performance. *J Control Release* 127:79–87.
- Ho L, Müller R, Gordon KC, Kleinebudde P, Pepper M, Rades T, Shen Y-C, Taday PF, Zeitler JA. 2009. Terahertz pulsed imaging as an analytical tool for sustained-release tablet film coating. *Eur J Pharm Biopharm* 71:117–123.
- Spencer JA, Gao Z, Morre T, Buhse LF, Taday PF, Newnham DA, Shen Y, Portieri A, Husain A. 2008. Delayed release tablet dissolution related to coating thickness by terahertz pulsed imge mapping. *J Pharm Sci* 97:1543–1550.
- Felton LA, Perry WL. 2002. A novel technique to quantify film-tablet interfacial thickness. *Pharm Dev Technol* 7:43–47.
- Shah RB, Tawakkul MA, Khan MA. 2007. Process analytical technology: Chemometric analysis of Raman and near infra-red spectroscopic data for predicting physical properties of extended release matrix tablets. *J Pharm Sci* 96:1356–1365.
- Roggo Y, Jent N, Edmond A, Chalus P, Ulmschneider M. 2005. Characterizing process effects on pharmaceutical solid forms using near-infrared spectroscopy and infrared imaging. *Eur J Pharm Biopharm* 61:100–110.
- Andersson M, Josefson M, Langkilde FW, Wahlund KG. 1999. Monitoring of a film coating process for tablets using near infrared reflectance spectrometry. *J Pharmaceut Biomed* 20:27–37.
- Moes JJ, Ruijken MM, Gout E, Frijlink HW, Ugwoke MI. 2008. Application of process analytical technology in tablet process development using NIR spectroscopy: Blend uniformity, content uniformity and coating thickness measurements. *Int J Pharm* 357:108–118.
- Buchanan BR, Baxter MA, Chen TS, Qin XZ, Robinson PA. 1996. Use of near-infrared spectroscopy to evaluate an active in a film coated tablet. *Pharm Res* 13:616–621.
- El Hagrasy AS, Chang S, Desai D, Kiang S. 2006. Raman spectroscopy for the determination of coating uniformity of tablets: Assessment of product quality and coating pan mixing efficiency during scale-up. *J Pharm Inn* 1:37–42.
- Zannikos PN, Li WI, Drennen JK, Lodder RA. 1991. Spectrophotometric prediction of the dissolution rate of carbamazepine tablets. *Pharm Res* 8:974–978.
- Donoso M, Ghaly ES. 2004. Prediction of drug dissolution from tablets using near-infrared diffuse reflectance spectroscopy as a nondestructive method. *Pharm Dev Technol* 9:247–263.
- Freitas MP, Sabadin A, Silva LM, Giannotti FM, do Couto DA, Tonhi E, Medeiros RS, Coco GL, Russo VFT, Martins JA. 2005. Prediction of drug dissolution profiles from tablets using NIR diffuse reflectance spectroscopy: A rapid and nondestructive method. *J Pharmaceut Biomed* 39:17–21.
- Otsuka M, Tanabe H, Osaki K, Otsuka K, Ozaki Y. 2007. Chemoinformetrical evaluation of dissolution property of indomethacin tablets by near-infrared spectroscopy. *J Pharm Sci* 96:788–801.
- Kirsch JD, Drennen JK. 1995. Determination of film-coated tablet parameters by near-infrared spectroscopy. *J Pharm Biomed* 13:1273–1281.
- Barbash D, Fulghum JE, Yang J, Felton LA. 2009. A novel imaging technique to investigate the influence of atomization air pressure on film-tablet interfacial thickness. *Pharm Dev Technol* 35:480–486.
- Fitzgerald AJ, Cole BE, Taday PF. 2005. Nondestructive analysis of tablet coating thicknesses using terahertz pulsed imaging. *J Pharm Sci* 94:177–183.

21. Zeitler JA, Shen Y, Baker C, Taday PF, Pepper M, Rades T. 2007. Analysis of coating structures and interfaces in solid oral dosage forms by three dimensional terahertz pulsed imaging. *J Pharm Sci* 96: 330–340.
22. Ho L, Müller R, Römer M, Gordon KC, Heinämäki J, Kleinebudde P, Pepper M, Rades T, Shen Y-C, Strachan CJ, Taday PF, Zeitler JA. 2007. Analysis of sustained-release tablet film coats using terahertz pulsed imaging. *J Control Release* 119:253–261.
23. Shen YC, Taday PF, Newnham DA, Kemp MC, Pepper M. 2005. 3D chemical mapping using terahertz pulsed imaging. *Proceedings of SPIE-The International Society for Optical Engineering* 572. (Terahertz and Gigahertz Electronics and Photonics IV): 24–31.
24. Zeitler JA, Taday PF, Newnham DA, Pepper M, Gordon KC, Rades T. 2007. Terahertz pulsed spectroscopy and imaging in the pharmaceutical setting—A review. *J Pharm Pharmacol* 59:209–223.
25. Shen YC, Taday PF. 2008. Development and application of terahertz pulsed imaging for nondestructive inspection of pharmaceutical tablet. *IEEE J Quantum Elect* 14:1–9.
26. Ho L, Müller R, Gordon KC, Kleinebudde P, Pepper M, Rades T, Shen Y-C, Taday PF, Zeitler JA. 2008. Investigating dissolution performance critical area on coated tablets: A case study using terahertz pulsed imaging. Submitted to *Journal of Pharmaceutical Sciences*.
27. Banakar UV, Lathia CD, Wood JH. 1992. Interpretation of dissolution rate data and techniques of in vivo dissolution. In: Banakar UV, editor. *Pharmaceutical dissolution testing*. 1st edition. New York: Marcel Dekker Inc. pp. 189–249.
28. Rinaki E, Dokoumetzidis A, Macheras P. 2003. The mean dissolution time depends on the dose/solubility ratio. *Pharm Res* 20:406–408.
29. Eriksson L, Johansson E, Kettaneh-Wold N, Trygg J, Wikström C, Wold S. 2006. Multi- and megavariate data analysis part I: Basic principles and applications. 2nd edition. Umeå: Umetrics AB. pp. 63–219.
30. Esbensen KH. 2006. *Multivariate data analysis—In practice*. 5th edition. Oslo: Camo Software AS. pp. 19–270.
31. Wold S, Sjöström M, Eriksson L. 2001. PLS-regression: A basic tool of chemometrics. *Chemometr Intell Lab* 58:109–130.